GEOPHYSICAL RESEARCH LETTERS, VOL. 36, L01302, doi:10.1029/2008GL036068, 2009

Three-dimensional fold structure of the Tibetan Moho from GRACE gravity data

Young Hong Shin,[1] C.-K. Shum,[2] Carla Braitenberg,[3] Sang Mook Lee,[4] Houze Xu,[5] Kwang Sun Choi,[6] Jeong Ho Baek,[1] and Jong Uk Park[1]

Received 19 September 2008; revised 17 November 2008; accepted 4 December 2008; published 6 January 2009.

[1] Although the prevailing wavelength of the Moho fold has been estimated from the spectral analysis of gravity and topography, there has not been a suggested method developed to reveal its structure. Here we present a three-dimensional (3D) Moho fold structure beneath Tibet which clearly reflects the continental collision. For the structure estimation a new method has been introduced based on the gravity inversion and flexural model. The estimated direction and wavelength of the Moho fold are consistent with the velocities calculated from Global Positioning System (GPS) and with an elastic plate model under horizontal compression. The prevailing wavelength of the Moho fold is estimated to be 300 to 420 km, which corresponds to an elastic plate with effective elastic thickness (EET) of about 35 km, and much smaller than the prior estimates of 500 to 700 km. **Citation:** Shin, Y. H., C.-K. Shum, C. Braitenberg, S. M. Lee, H. Xu, K. S. Choi, J. H. Baek, and J. U. Park (2009), Three-dimensional fold structure of the Tibetan Moho from GRACE gravity data, *Geophys. Res. Lett.*, *36*, L01302, doi:10.1029/2008GL036068.

1. Introduction

[2] The Tibetan Plateau, the world's highest and biggest plateau, is thought to have been formed resulting from the collision of the two continental plates, the Eurasian and Indian plates. Due to the high topography and active compressional forces, it is expected that Tibet should have an extraordinarily thick crust and its Moho should be buckled [e.g., *Jin et al.*, 1996]. Substantial geophysical studies have been conducted to reveal the structure of crust and mantle beneath the plateau and the associated geologic history. The crustal structure has been studied by several seismic exploration campaigns [e.g., *Kind et al.*, 2002; *Haines et al.*, 2003; *Vanderhaeghe and Teyssier*, 2001; *Kind et al.*, 1996; *Nelson et al.*, 1996]. However, these investigations were carried out only along a few cross-sectional lines, the extension of which is insufficient to fully describe the Moho structure, as only a small fraction of the plateau is covered. Only a few studies using gravimetric inversion [e.g., *Braitenberg et al.*, 2000a, 2000b] and flexural model [e.g., *Braitenberg et al.*, 2003; *Jin et al.*, 1996; *Caporali*, 2000; *Lyon-Caen and Molnar*, 1983] for the Tibetan plateau and surrounding regions are available, which are hampered by limited data coverage due to precipitous and remotely approachable topography. Recently *Shin et al.* [2007] presented a Moho undulation model that covered the whole plateau and surrounding areas, overcoming the geographical limitation by adopting the modern satellite-based combination gravity model, GGM02C [*Tapley et al.*, 2005]. In describing the particular features of the Moho undulation, they identified the "Moho ranges" a mountain range-like structure on Moho that keeps semi-regular interval between ranges. The existence of a buckling structure of the Moho beneath Tibet has been discussed by *Jin et al.* [1994] who estimated the dominant wavelength to be about 500–700 km based on the method of spectral analysis of gravity and topography data. The three-dimensional (3D) structure of the Moho fold, however, has not been estimated nor a method to explain it been suggested until now.

[3] We present a new method to estimate the 3D fold structure of Moho and an improved geophysical quantification. The method is based on the principle of comparing the current Moho obtained from gravity inversion with the crustal thickness variations expected for a flexural or local isostatic model. The gravity anomaly due to the undulation of the Moho is estimated from the recently available improved gravity model, EIGEN-GL04C [*Förste et al.*, 2007], which is combined data from the GRACE (Gravity Recovery and Climate Experiment) mission [*Tapley et al.*, 2004] and other data including terrestrial gravimetry. The resulting Moho fold model is found to be consistent with the current observed horizontal crustal velocities as measured by Global Positioning System (GPS) [*Gan et al.*, 2007] and with the predicted wavelength of the fold formation from an elastic plate under horizontal compression. The predominant wavelength of the fold is estimated to be about 300–420 km, substantially different with the previous estimated values [*Jin et al.*, 1994].

2. Methodology of Moho Fold Estimation

[4] Fold structures, exposed on the surface or presented in shallow subsurface strata, can be obtained by direct observation or geologic-geophysical investigations. Constraining the fold structure of the Moho, however, which lies much deeper and in the Tibetan case at about 70 km depth, is a difficult task. Here we outline a methodology for estimating the 3D fold structure of the deep Moho beneath the Tibetan plateau that benefited from the newly available

[1]Korea Astronomy and Space Science Institute, Daejeon, South Korea.
[2]School of Earth Sciences, Ohio State University, Columbus, Ohio, USA.
[3]Department of Earth Sciences, University of Trieste, Trieste, Italy.
[4]School of Earth and Environmental Sciences, Seoul National University, Seoul, South Korea.
[5]Institute of Geodesy and Geophysics, Chinese Academy of Sciences, Wuhan, China.
[6]Department of Earth Science, Pusan National University, Pusan, South Korea.

0094-8276/09/2008GL036068$05.00

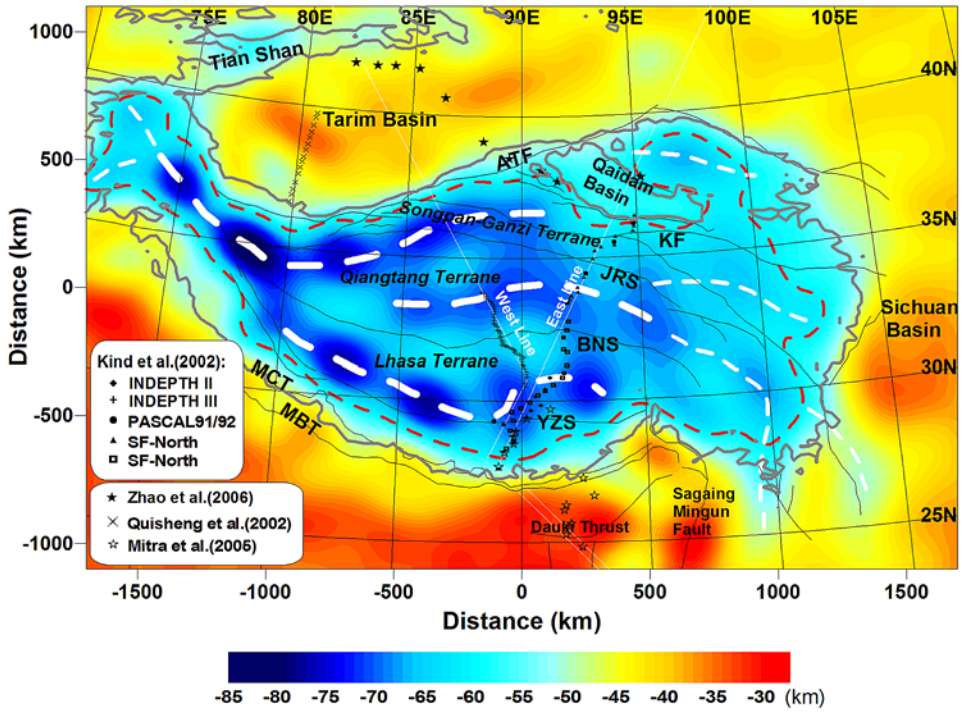

Figure 1. Moho undulation model derived from EIGEN-GL04C: abnormally deep Moho over 60 km is found inside the plateau (surrounded by red dashes), while the deepest Moho up to 83.2 km is found in western Tibet. Tectonic lines are labeled with acronyms as MBT (Main Himalaya Thrust), MCT (Main Central Thrust), YZS (Yarlung-Zangbo Suture), BNS (Bangong-Nujiang Suture), JRS (Jinsha River Suture), KF (Kunlun Fault), and ATF (Altyn Tagh Fault). Grey line represents 3-km-height level to outline the plateau. Various symbols and legends in the boxes are used to show the locations of seismic experiments. Profiles along two white lines, designed to compare with seismic experiments, are given in Figure S5.

global gravity field model. We begin with the traditional theory of isostasy and gravity inversion to define the current status of crustal thickening. We assume that the undulations of the Moho are mainly caused by vertical and horizontal loadings, which result in isostatic crustal thickening and buckling (folding), respectively. Both the Airy-type isostatic and flexural response are considered, with preference to the latter, as the former assumes the unrealistic zero rigidity value of the lithosphere. The numerous other geophysical conditions are beyond our study scope, not only because they are hard to be modeled but because they do not significantly alter our assumption. We thus suggest that the deviation of the current Moho from the isostatic equilibrium can be largely explained by the fold structure in a collision environment, where the horizontal compression is the dominant force. The direction and wavelength of the estimated Moho fold (buckling) could then be validated by comparison with GPS observations and an elastic plate model under horizontal compression. Our methodology is described in detail in the auxiliary material.[1]

3. Fold Structure of Moho

[5] The existence of Moho fold and its dominant wavelengths had already been investigated. *Jin et al.* [1994] suggested that the prevailing buckling occurred at two wave bands centered around 150–200 km (upper crust) and 500–700 km (upper mantle) in Tibet. *Caporali* [2000] estimated that the lithosphere folded at wavelengths near 250 km in the western Himalaya and Karakoram. On the other hand, *Burov et al.* [1993] thought that the structures of 300–360 km were caused by buckling of upper mantle layer having EET of 40–70 km in the western Gobi.

[6] We investigate if the Moho fold components can be determined by analyzing the manner in which the Moho model deviates from isostatic equilibrium, both in the cases of local isostasy and flexural model. To estimate the current status of Moho undulation using gravity data, we follow the data processing methods of *Shin et al.* [2007] and the result is shown in Figure 1. In this study however the most recent GRACE-combination gravity model (GRACE data combined with LAGEOS satellite laser ranging tracking data, terrestrial gravimetry and altimetry data, and complete to spherical harmonic degree 360), the EIGEN-GL04C model [*Förste et al.*, 2007], is used instead of the GGM02C model [*Tapley et al.*, 2005] and the EGM96 model [*Lemoine et al.*, 1998].

[7] We can obtain a preliminary fold structure from the deviation of the Moho model from the Airy-type isostasy (Figure S7). From the preliminary result one can identify the directional trend which is parallel to the Tibetan border and main tectonic lines, which extend to the border and over the nearby surrounding areas of the plateau. The directional trends were already found in the Moho model, but were only confined to the inside of the plateau [*Shin et al.*, 2007]. Our study however suggests that Airy-type isostasy is inadequate in explaining the fold structure, as it failed to

[1] Auxiliary materials are available in the HTML. doi:10.1029/2008GL036068.

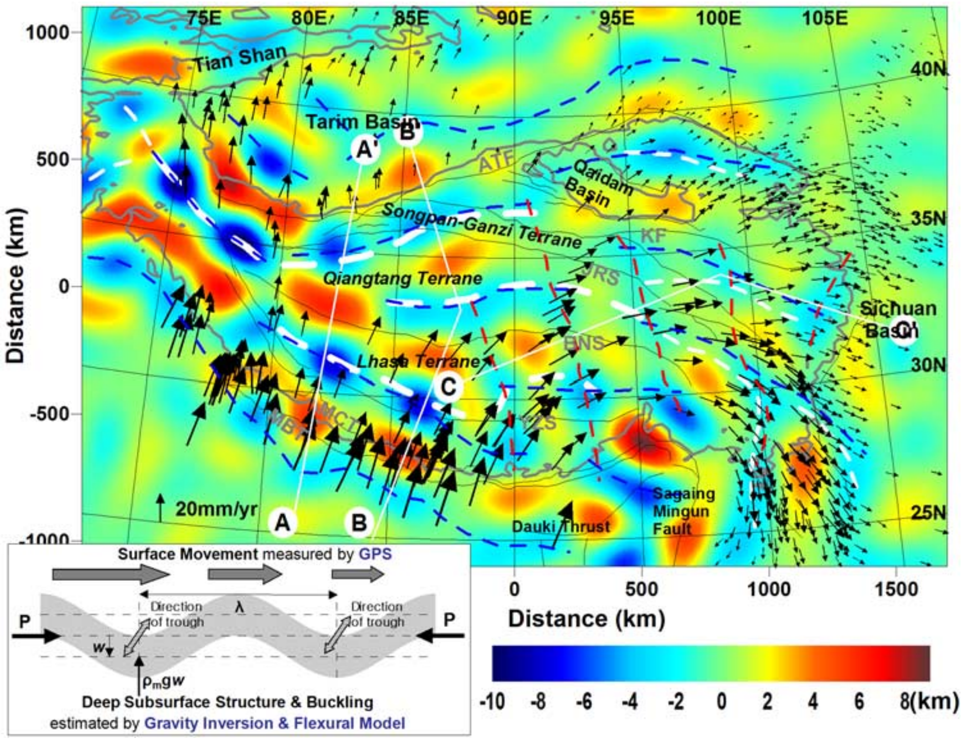

Figure 2. Moho fold structure and surface movement from GPS: blue dashed lines denote E-W directional fold troughs and red ones N-S directional troughs. Moho ranges, white dashed lines [*Shin et al.*, 2007] are shown for comparison. Blank arrows represent surface movement from GPS data [*Gan et al.*, 2007]. Cross-sections along AA′, BB′ and CC′ are presented in Figures 4 and S8. Schematic illustration of Moho fold estimation is shown in lower left inset.

manifest the N-S directional strike of the Moho fold in eastern Tibet, which differs from the direction of prevailing crustal movement in E-W.

[8] The more realistic way to explain the compensation appears to be the flexural model. This is normally done by calculating the EET from the spectral analysis of topography and Bouguer gravity anomaly. We applied a flexure response filter shown in Figure 3, which corresponds to an average EET of 35 km based on the analysis of *Shin et al.* [2007]. The final Moho fold structure is shown in Figure 2, which now reveals the presence of both E-W and N-S trending structures. The amplitude of the Moho fold varies from −10.14 km to 9.59 km with a standard deviation of 2.04 km. The structures seem to be in good agreement with the Moho ranges reported by *Shin et al.* [2007] except for a small region in eastern Tibet. The intervals between the fold troughs appear to be considerably regular (Figure 2), which suggests that the lateral variation of rigidity may be small. One notable feature is that the dominant direction of the strike of the fold changes from an E-W direction in western Tibet to a N-S direction in eastern Tibet. If one simply takes the amplitudes of the fold as the overall strength of the tectonic force, the strongest force seems to have been applied to the southern border and western Tibet. Since the compressional stress should have acted perpendicular to the structures, we find that the azimuth of the Moho folds correlate with that of the surficial shortening as revealed by recent GPS measurements of horizontal crustal velocities [*Gan et al.*, 2007].

[9] The prevailing wavelength is estimated to be 300–420 km from the power spectral analysis of the Moho folds (Figure 3). The prevailing wavelength from our results is consistent with that predicted by an elastic plate under horizontal compression; the wavelength for a simple elastic plate is estimated to be 368 km for EET of 35 km, and 328 km and 407 km for EET 30 km and 40 km, respectively (auxiliary material). *Shin et al.* [2007] reported that the splitting of Moho ranges happened as the distance between

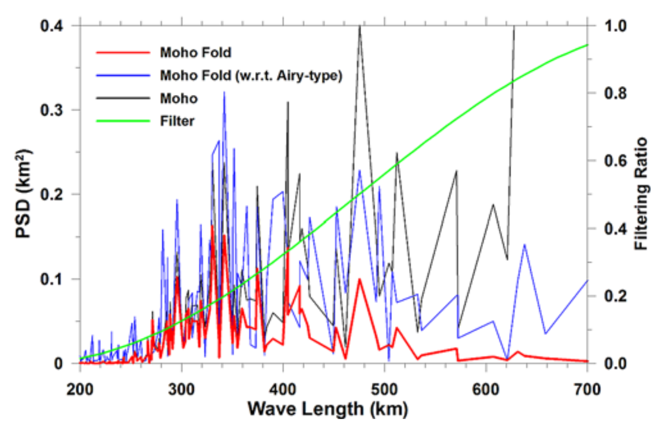

Figure 3. Power spectral density of the Moho and its fold models, and filter applied for flexural model: the red and blue lines represent final and preliminary Moho fold models, respectively. The dominant wavelengths of Moho fold are estimated to be about 300–420 km (peaks at 295, 330, 342, 374, 405, and 418 km). Filter is designed to fit well with observed coherence between gravity and topography.

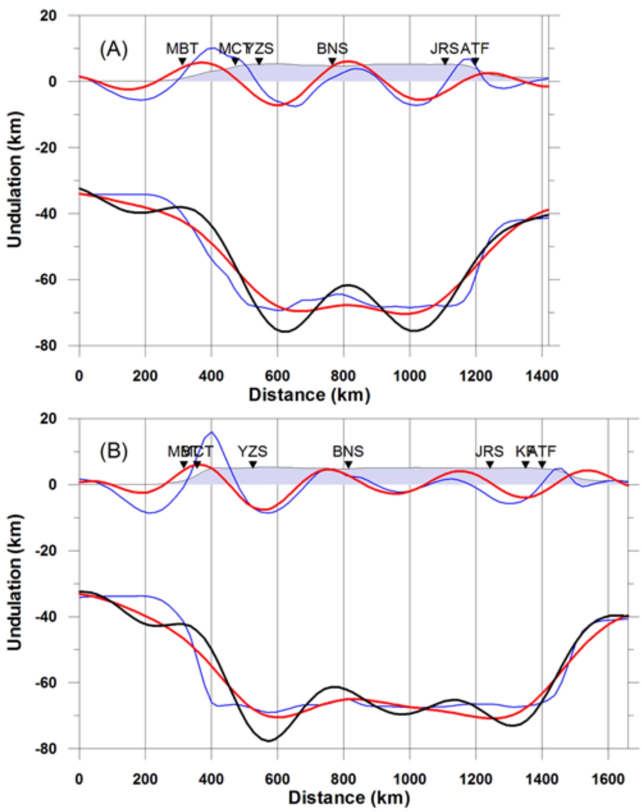

Figure 4. Cross-sectional view along AA′ and BB′: upper black line with shadow denotes topography. Lower black, red and blue lines denote Moho models based on gravity inversion, flexural model and local isostasy, respectively. Upper red and blue lines show Moho fold undulations based on flexural and local isostasy models, respectively. Inverse triangles represent cross-over points with tectonic lines.

them increases over about 330 km. The prevailing wavelength estimated here could explain the reason of the splitting and the origin of the Moho ranges. Though the wavelengths greater than 420 km could have been also affected and deformed by compression, they are thought to have largely originated from isostatic compensation. For example, a long wavelength of 475 km can be seen in the spectrum. It is however unclear in Figure 2 if such a long wavelength feature exists, except for the narrow area in the north-eastern end of the plateau. This wavelength corresponds to an EET of about 50 km, much greater than that of the estimated one, i.e., 35 km for the plateau.

[10] The profiles in Figures 4 and S8 correspond to the three cross-lines in Figure 2. The Moho fold undulations along line AA′ and BB′ which cut across the E-W directional buckling show that they have constant amplitude and wavelength of about 400 km, while the amplitude outside the plateau diminishes rapidly. Such observation can be considered as resulting from the relaxation of stress due to the subduction of outside plates. The amplitude along profile CC′ (Figure S8) which transects the N-S trending buckling structure is found to be much smaller than features along AA′ and BB′ (Figure 4). This difference can be interpreted as showing that the E-W directional compression is smaller than that of N-S directional which can be also seen in the GPS horizontal velocities (Figure 2). The wavelength along CC′ is slightly smaller than those along AA′ and BB′, which may indicate the smaller EET in eastern Tibet compared to western Tibet. Such feature may be related with upper crustal cracks, crustal decoupling or may have been caused by an anomalous geothermal environment.

4. Concluding Remarks

[11] We have quantified the 3D Tibetan Moho fold structure and presented the new methodology of its determination that is based on gravity inversion and flexural consideration. We then validated the resulting Moho fold model by comparing it with GPS velocities and with an elastic plate of same EET both in direction, amplitude, and wavelength. As described above features of our Moho fold model can be summarized as follows: (a) E-W directional trend is prominent in western Tibet, while N-S directional trend in eastern Tibet, (b) the fold structures are not limited into the inside of the plateau but extended to the near surroundings of the plateau, (c) the amplitude of the fold is up to about 10 km (−9.87 to 8.83 km) inside the plateau, (d) the amplitude decreases rapidly outside the plateau, (e) the intervals between the fold troughs are observed to keep considerably a regular distance of about 300–420 km, which is close to the predicted values using an elastic plate model, and (f) our model is in good agreement with the recent GPS measured horizontal velocities.

[12] The existence of partial melting [*Vanderhaeghe and Teyssier*, 2001; *Kind et al.*, 1996; *Nelson et al.*, 1996] which makes the lithosphere less strong and reduces the EET [*Shin et al.*, 2007; *Braitenberg et al.*, 2003; *Jin et al.*, 1996; *Caporali*, 2000] could support the existence of Moho fold. In addition, the areas near the Himalayan syntaxis around (80E, 34N) and (95E, 28N) show a break in the structure like a broken bow and large amplitude of Moho fold, which lead us to expect huge stress and differential movement although there is no available GPS observation in the region. We find a rather poor correlation between the direction of the Moho folds and the GPS observed crustal velocity in the southeast of the study area. The lack of correlation appears to support the idea of decoupling of the lithosphere as it could be interpreted that the upper crustal mass has been decoupled and is flowing in a southeast direction, not representing the deeper lying structures. Finally, the concept and analysis of Moho ranges and fold structure would be useful for improving our understanding of the geologic history of the Tibetan Plateau.

[13] **Acknowledgments.** We thank the two anonymous reviewers for their constructive comments and valuable suggestions, which have improved the paper. The gravity field models used in this study are provided by GeoForschungsZentrum (GFZ) Potsdam, University of Texas Center for Space Research, National Geospatial-Intelligence Agency (NGA), and Universitaet Bonn. The research conducted in the US is supported by grants from NASA (NNG04GN19G and NNG04GF01G) and from NSF under the Collaboration in Mathematical Geosciences (CMG) Program (EAR0327633).

References

Braitenberg, C., M. Zadro, J. Fang, Y. Wang, and H. T. Hsu (2000a), Gravity inversion in Qinghai-Tibet Plateau, *Phys. Chem. Earth*, *25*, 381–386.

Braitenberg, C., M. Zadro, J. Fang, Y. Wang, and H. T. Hsu (2000b), The gravity and isostatic Moho undulations in Qinghai-Tibet Plateau, *J. Geodyn.*, *30*, 489–505.

Braitenberg, C., Y. Wang, J. Fang, and H. Y. Hsu (2003), Spatial variations of flexure parameters over the Tibet-Qinghai Plateau, *Earth Planet. Sci. Lett.*, *205*, 211–224.

Burov, E. B., L. I. Lobkovsky, S. Sloetingh, and A. M. Nikishin (1993), Continental lithosphere folding in central Asia. II: Constraints from gravity and topography, *Tectonophysics*, *226*, 73–87.

Caporali, A. (2000), Buckling of the lithosphere in western Himalaya: Constraints from gravity and topography data, *J. Geophys. Res.*, *105*, 3103–3113.

Förste, C., et al. (2007), The GeoForschungsZentrum Potsdam/Groupe de Recherche de Geodesie Spatiale satellite-only and combined gravity field models: EIGEN-GL04S1 and EIGEN-GL04C, *J. Geod.*, *82*, 331–346.

Gan, W., P. Zhang, Z.-K. Shen, Z. Niu, M. Wang, Y. Wan, D. Zhou, and J. Cheng (2007), Present-day crustal motion within the Tibetan Plateau inferred from GPS measurements, *J. Geophys. Res.*, *112*, B08416, doi:10.1029/2005JB004120.

Haines, S. S., S. L. Klemperer, L. Brown, J. Guo, J. Mechie, R. Meissner, A. Ross, and W. Zhao (2003), INDEPTH III seismic data: From surface observations to deep crustal processes in Tibet, *Tectonics*, *22*(1), 1001, doi:10.1029/2001TC001305.

Jin, Y., M. K. McNutt, and Y. Zhu (1994), Evidence from gravity and topography data for folding of Tibet, *Science*, *371*, 669–674.

Jin, Y., M. K. McNutt, and Y. Zhu (1996), Mapping the descent of Indian and Eurasian plates beneath the Tibetan Plateau from gravity anomalies, *J. Geophys. Res.*, *101*, 11,275–11,290.

Kind, R., J. Ni, W. Zhao, J. Wu, X. Yuan, L. Zhao, E. Sandvol, C. Reese, J. Nabelek, and T. Hearn (1996), Evidence from earthquake data for a partially molten crustal layer in southern Tibet, *Science*, *274*, 1692–1694.

Kind, R., et al. (2002), Seismic images of crust and upper mantle beneath Tibet: Evidence for Eurasian plate subduction, *Science*, *298*, 1219–1221.

Lemoine, F. G., et al. (1998), The development of the joint NASA GSFC and the NIMA geopotential model EGM96, *NASA/TP-1998-206,861*, NASA Goddard Space Flight Cent., Greenbelt, Md.

Lyon-Caen, H., and P. Molnar (1983), Constraints on the structure of the Himalaya from an analysis of gravity anomalies and a flexural model of the lithosphere, *J. Geophys. Res.*, *88*, 8171–8191.

Mitra, S., K. Priestley, A. Bhattacharyya, and V. K. Gaur (2005), Crutsal structure and earthquake focal depths beneath northeastern India and southern Tibet, *Geophys. J. Int.*, *160*, 227–248.

Nelson, K. D., et al. (1996), Partially molten middle crust beneath southern Tibet: Synthesis of project INDEPTH results, *Science*, *274*, 1684–1688.

Qiusheng, L., G. Rui, L. Deyuan, L. Jingwei, F. Jingyi, Z. Zhiying, L. Wen, L. Yingkang, Y. Quanren, and L. Dexing (2002), Tarim underthrust beneath western Kunlun: Evidence from wide-angle seismic sounding, *J. Asian Earth Sci.*, *20*, 247–253.

Shin, Y. H., H. Xu, C. Braitenberg, J. Fang, and Y. Wang (2007), Moho undulations beneath Tibet from GRACE-integrated gravity data, *Geophys. J. Int.*, *170*, 971–985.

Tapley, B., S. Bettadpur, J. Ries, P. Thompson, and M. Watkins (2004), GRACE measurements of mass variability in the Earth system, *Science*, *305*, 503–505.

Tapley, B., et al. (2005), GGM02—An improved Earth gravity field model from GRACE, *J. Geod.*, *79*, 467–478.

Vanderhaeghe, O., and C. Teyssier (2001), Partial melting and flow of orogens, *Tectonophysics*, *342*, 451–472.

Zhao, J., W. D. Mooney, Z. Xiankang, L. Zhichun, J. Zhijun, and N. Okaya (2006), Crustal structure across the Altyn Tagh Range at the northern margin of the Tibetan Plateau and tectonic implications, *Earth Planet. Sci. Lett.*, *241*, 804–814.

J. H. Baek, J. U. Park, and Y. H. Shin, Korea Astronomy and Space Science Institute, Yuseong-gu, Daejeon 305-348, South Korea. (llamb@kasi.re.kr; jupark@kasi.re.kr; yhshin@kasi.re.kr)

C. Braitenberg, Department of Earth Sciences, University of Trieste, Via Weiss 1, I-34100 Trieste, Italy. (berg@units.it)

K. S. Choi, Department of Earth Science, Pusan National University, Geumjeong-gu, Pusan 609-735, South Korea. (ksunchoi@pnu.edu)

S. M. Lee, School of Earth and Environmental Sciences, Seoul National University, Sillim-dong, Gwanak-gu, Seoul 151-747, South Korea. (smlee@snu.ac.kr)

C.-K. Shum, School of Earth Sciences, Ohio State University, 470 Hitchcock Hall, Columbus, OH 43210, USA. (ckshum@osu.edu)

H. Xu, Institute of Geodesy and Geophysics, Chinese Academy of Sciences, 54 Xudong Road, Wuhan 130077, China. (hsuh@asch.whigg.ac.cn)